# Nanocomposites by Electrostatic Interactions: 1. Impact of Sublayer Quality on the Organization of Functionalized Nanoparticles on Charged Self-Assembled Layers

Frank Auer,[†] Michael Scotti,[‡] Abraham Ulman,*[,‡] Rainer Jordan,[‡,§] Börje Sellergren,*[,†] Jayne Garno,[||] and Gang-Yu Liu[||]

*Institut für Anorganische Chemie und Analytische Chemie, Johannes Gutenberg-Universität Mainz, Duesbergweg 10-14, 55099 Mainz, Germany, Department of Chemical Engineering and Chemistry and The NSF-MRSEC for Polymers at Engineered Interfaces, Polytechnic University, Six Metrotech Center, Brooklyn, New York 11201, and Department of Chemistry, Wayne State University, Detroit, Michigan 48202*

*Received May 3, 2000*

Bis-benzamidines were studied as linkers for the formation of gold nanoparticle assemblies on planar gold surfaces modified with $\omega$-mercaptohexadecanoic acid. In situ ellipsometry, external reflection Fourier transform spectroscopy, and atomic force microscopy showed that the packing density and order of the bis-benzamidine layer exerted a pronounced influence on the thickness and density of the nanoparticle layers. These layers exhibited optical properties similar to those of solid gold.

The control of size, shape, physical and chemical properties (e.g., stability, solubility, optical properties, surface functional groups, etc.) of nanoparticles at a *molecular level* is crucial to the fine-tuning of their electronic and optical behavior,[1] as well as to their further hierarchical self-organization into nanoassemblies.[2] One way to incorporate particles in complex assemblies is through electrostatic interactions.[3] These electrostatic forces that are carried by a protective organic layer, and by an intermediate linker molecule, are strong enough to ensure a sufficient stability of the assembly, yet weak enough to allow a reaction of the system to environmental changes, such as ionic strength or pH.

Here, we present a first account of such a system, based on studies on the preparation of well-defined thiol-functionalized gold nanoparticles,[4] and studies on pH-switchable self-assembled monolayers (SAMs).[5,6] In the latter we showed that the bis-benzamidine bolaamphiphiles, bearing different alkyl spacers, assemble on various SAMs of $\omega$-mercaptoalkanoic acids into stable, ordered, and moreover pH-switchable layers.

In this work we have investigated bis-benzamidines as positively charged linkers for the formation of nanoparticle assemblies of negatively charged $\omega$-mercaptoundecanoic acid (MUA) functionalized gold nanoparticles[7] onto $\omega$-mercaptohexadecanoic acid (MHA) SAMs deposited on gold. By variation of the intermediate alkyl chain length of the bis-benzamidine from pentamidine (PAM), to octamidine (OAM) and to dodecamidine (DODAM), the total surface charge density and stability of the intermediate double charged linker can be controlled, which results in potentially tunable and switchable properties of the entire assembly (Figure 1).

After deposition of complete MHA SAMs onto the native gold,[8] the adsorption of the bis-benzamidines PAM, OAM, and DODAM in a pH 9 buffer solution and the subsequent adsorption of the negatively charged gold clusters onto the positive amidine-surface were monitored in real time by in situ ellipsometry. The resulting optical thickness values of the amidine layers were in close agreement with previously reported ones,[6] with PAM giving a thickness corresponding to less than a monolayer, OAM close to a monolayer, and DODAM close to a bilayer, assuming an

[†] Johannes Gutenberg-Universität Mainz.

[‡] Polytechnic University.

[§] Present address: Lehrstuhl für Makromolekulare Stoffe, Institut für Technische Chemie, Technische Universität München, Lichtenbergstr. 4, D-85747 Garching, Germany.

[||] Wayne State University.

(1) Alivisatos, A. P. *Science* **1996**, *271*, 933−936. (b) Schmid, G. *Chem. Rev.* **1992**, *92*, 1709−1727. (c) Brust, M.; Walker M.; Bethell D.; Schiffrin D. J.; Whyman R. *J. Chem. Soc., Chem. Commun.* **1994,** 801. (d) Hostetler, M. J.; Wingate J. E.; Zhong, C. J.; Harris, J. E.; Vachet, R. W.; Clark, M. R.; Londono, J. D.; Green, S. J.; Stokes, J. J.; Wignall, G. D.; Glish, G. L.; Porter, M. D.; Evans, N. D.; Murray, R. W. *Langmuir* **1998**, *14*, 17−30 and references therein.

(2) Fendler, J. H., Ed. *Nanoparticles and Nanostructured Films*; Wiley-VCH: Weinheim, 1998. (b) Special Issue on Nanostructured Materials. *Chem. Mater.* **1996**, *8*. (c) Brust, M.; Bethell, D.; Schiffrin, D. J.; Kiely, C. J. *Adv. Mater.* **1995**. (d) Fitzmaurice, D.; Rao, S. N.; Preece, J. A.; Stoddart, J. F.; Wenger, S.; Zaccheroni, N.; *Angew. Chem., Int. Ed. Engl.* **1999**, *38*, 1147−1150.

(3) Schmitt, J.; Decher, G.; et al. *Adv. Mater.* **1997**, *9*, 61. (b) Schmitt, J.; Mächtle, P.; Eck, D.; Möhwald, H.; Helm, C. A. *Langmuir* **1999**, *15* (9), 3256 and references therein. (c) Loweth, C. J.; Caldwell, W. P.; Peng, X.; Alivisatos, A. P.; Schultz, P. G. *Angew. Chem. Int. Ed.* **1999**, 38, 1808.

(4) Yee, C. K.; Jordan, R.; Ulman, A.; White, H.; King, A.; Rafailovich, M.; Sokolov, J. *Langmuir* **1999**, *15* (10), 3486−3491.

(5) Sellergren, B.; Swietlow, A.; Arnebrant, T.; Unger, K. K. *Anal. Chem.* **1996**, *68*, 402−407.

(6) Auer, F.; Schubert, D. W.; Stamm, M.; Arnebrant, T.; Swietlow, A.; Zizlsperger, M.; Sellergren, B. *Chem Eur. J.* **1999**, *5*, 1150−1159.

(7) The procedure of Johnson et al.[7b] was modified for alkyl carboxcylic acid thiols and was as follows: In a 250 mL flask, 1 mmol of hydrogen tetrachloroaurate trihydrate was added to 20 mL of methanol, resulting in a pale gold colored solution. Next, 20 mL of a colorless 0.0715 M solution of COOH−$C_{10}$−SH (mercaptoundecanoic acid) was added, upon which the color turned from yellow-gold to a cloudy, opaque, dark yellow-brown after 30 s. Next, 10 mL of acetic acid was added, with no color change observed. This solution was stirred for 10 min and then was reduced by slow addition of a 0.89 M solution of sodium borohydride to the flask. Upon addition of the reducing agent, solution turned immediately black, indicating the formation of the gold nanoparticles. The solution was left to stir for 3 h more. The solvent was then evaporated to approximately 10 mL, and the black residue was washed with diethyl ether three times to remove free thiol. Next, the residue was washed three times with water and then with methanol and put to dry on a vacuum line with heat overnight. (b) Johnson, S. R.; Evans, S. D.; Brydson, R. *Langmuir* **1998**, *14*, 6639−6647

(8) Planar gold substrates were prepared according to: Jordan, R.; Ulman, A. *J. Am. Chem. Soc.* **1998**, *120*, 243−247. The MHA SAMs were prepared according to ref 6.

10.1021/la000647x CCC: $19.00 
Published on Web 08/26/2000

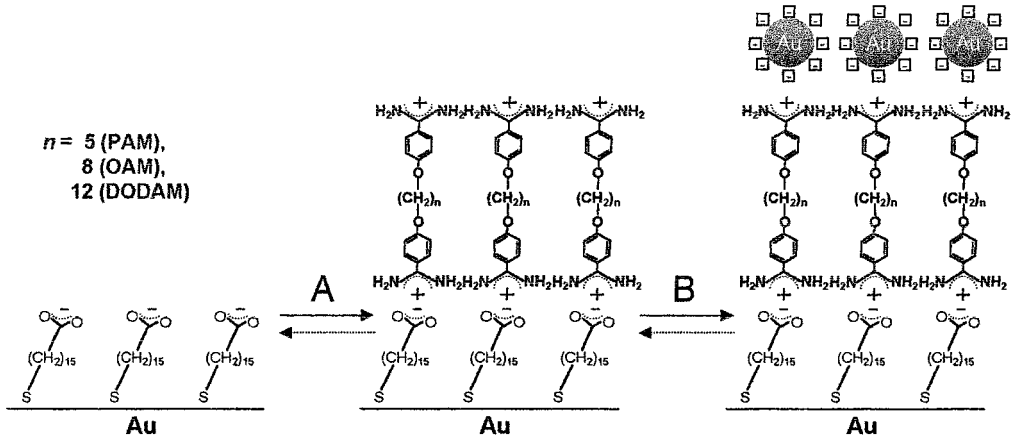


**Figure 1.** Schematic representation of the consecutive build-up of a SAM/nanoparticle composite by means of electrostatic interactions. Three different bis-benzamidines were used to serve as linking layers, $n = 5$ pentamidine (PAM), $n = 8$ octamidine (OAM), and $n = 12$ dodecamidine (DODAM).

**Table 1. Optical Constants and Layer Thickness ($d$) of Native and Modified Substrates[a]**

| modification | optical constants of unmodified gold, $n - j(k)$ | MHA layer, $d$ (nm) | benzamidine layer, $d$ (nm) | optical constants of particle layer, $n - j(k)$ | particle layer, $d$ (nm) |
|---|---|---|---|---|---|
| PAM | $0.2179 - j(3.1137)$ | 2.0 | 1.1 | $0.1817 - j(2.9216)$ | 2.4 |
| OAM | $0.1500 - j(3.0494)$ | 1.8 | 3.0 | $0.1712 - j(2.8882)$ | 7.7 |
| DODAM | $0.1728 - j(3.1309)$ | 2.0 | 5.2 | $0.1876 - j(2.8770)$ | 20.2 |

[a] See ref 9.

extended conformation of the molecules (molecular lengths were 2.1, 2.6, and 3.2 nm respectively, Table 1[9]). After adsorption equilibrium was reached, the bis-benzamidine solution was purged with pure buffer solution and replaced by a colloidal buffer solution of MUA-modified gold nanoparticles. The concentration of the MUA-modified gold nanoparticles in the buffer solution was 0.18 mg $mL^{-1}$. The kinetics curves for the adsorption on the three different amidine surfaces are displayed in Figure 2.

Similar to our previous results,[6] the different quality/order of the bis-benzamidine layers results in variations of the layer thickness of the charged nanoparticles. However, the differences in thickness of the particle layers are significant. On PAM, the least dense amidine layer, a final particle layer thickness of only 2.4 nm was measured. On comparison with the particle diameter of approximately $5.8 \pm 0.4$ nm (the gold core diameter is $2.9 \pm 0.4$ nm from transmission electron microscopy (TEM), and the thickness of the MUA shell is 2(1.7 nm) cos(30°)), this thickness corresponds to a submonolayer. On the other hand, OAM and DODAM gave particle layer thicknesses of 7.7 and 20.2 nm, respectively. Thus, regarding only the optical thickness readings, a layer in excess of one layer of particles was formed with OAM, while adsorption on DODAM resulted in the formation of more than three layers of particles. It is also apparent from the real time measurements that the better organized is the amidine layer, the faster is the adsorption kinetics. This trend can be correlated with the length of the amidine alkyl chain, which is the order-inducing mesogenic unit in the amidine SAM, controlling the charge density as well as stability of the linking layer toward exchange. When this layer becomes more ordered, particle−amidine interactions (Coulomb as well as H-bonding)[6] are optimized, thus allowing higher packing densities of the particles.

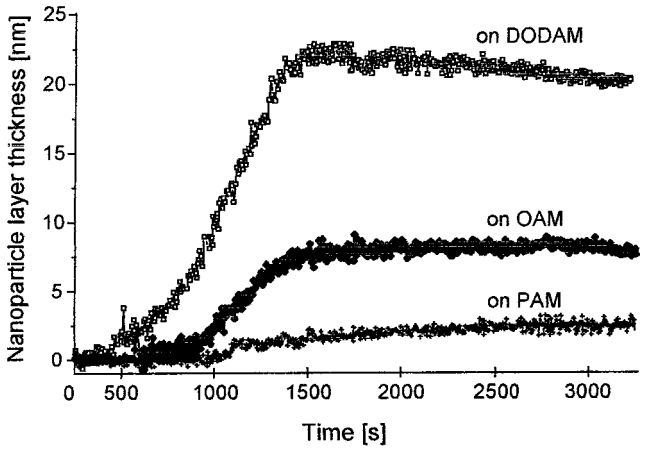


**Figure 2.** Real time change in layer thickness during the adsorption of MUA-modified gold nanoparticles on bis-benzamidine−MHA modified gold surfaces as measured by in situ ellipsometry (DRE-Ellipsometerbau, ELX-1 Precisionellipsometer; angle of incidence, 70°; HeNe laser, $\lambda = 632.8$ nm). (A) Bis-benzamidine (HCl or isethionate salt) stock solution (2.5 mM) was added into a Teflon cuvette filled with 2 mL borate buffer (pH 9) to reach a final concentration of 50 $\mu$M. (B) The gold nanoparticle solutions were prepared (3.7 mg/mL) by dissolving the acid-modified gold nanoparticles in 0.01 M sodium borate buffer solution (pH 9, adjusted with 0.1 M NaOH). After rinsing of the cell, a solution of modified gold nanoparticles was added to the well-stirred ellipsometric cuvette containing sodium borate buffer, reaching a final nanoparticle concentration of 0.0.18 mg/mL.

The morphologies of all three amidine layers were imaged using atomic force microscopy (AFM). The DODAM layer exhibits a distinct surface morphology, as shown in Figure 3a, flat, irregularly shaped domains with lateral dimensions from 10 to 200 nm and heights of $6.0 \pm 1.0$ nm. The measured height confirms the formation of a

(9) The thickness values for the MHA and bis-benzamidine layers were calculated using a refractive index of 1.45. Each value is the arithmetical mean value of 10 measurements on three individual spots of each substrate. Errors of given optical thickness were as follows: $d$(MHA) was ±0.2 nm, $d$(PAM, OAM, DODAM) was ±0.3 nm, and $d$(particle layer) was ±0.5 nm as estimated from the standard deviations.

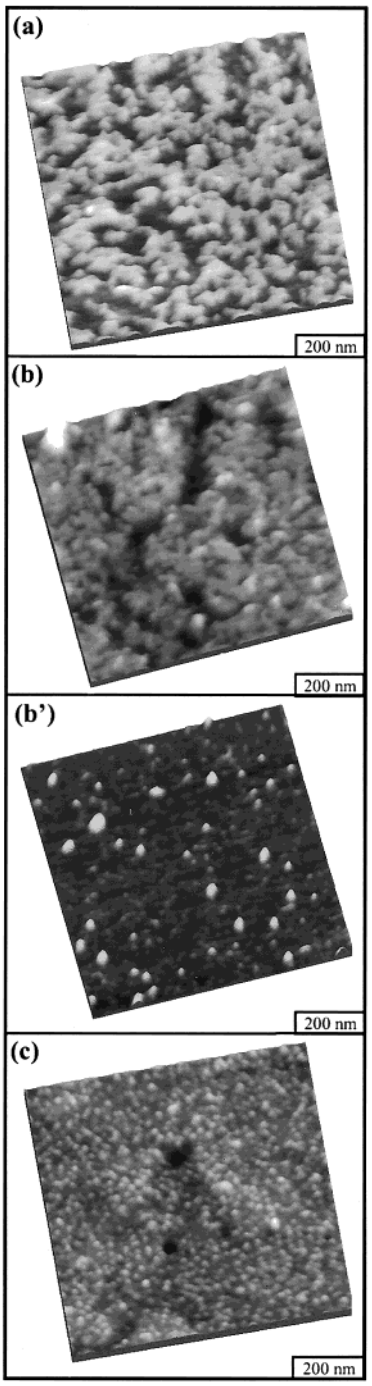


**Figure 3.** (a) Topographical AFM images (0.8 × 0.8 $\mu m^2$) of DODAM. (b) Topographical AFM images (0.8 × 0.8 $\mu m^2$) of DODAM bilayer after immersion in the gold nanoparticle solution for 4.5 h. Particle location is more easily identified in the corresponding elasticity image shown in panel b′, where the hard particles appear as bright spots. (c) Topographical AFM images (0.8 × 0.8 $\mu m^2$) of DODAM bilayer after immersion in the gold nanoparticle solution for 12 h. Particle concentration is 0.07 mg/mL.

bilayer of DODAM. Broad gaps are present, (dark areas) representing an uncovered SAM. The morphology of layers PAM and OAM are less homogeneous than the bilayer of dodecamidine partly due to the presence of three-dimensional clusters. The adsorption of MUA gold nanoparticles on the DODAM bilayers was also studied by monitoring the surface structure as a function of immersion time. The nanoparticle concentration was diluted to 0.07 mg/mL to slow the kinetics for detailed AFM investigations. Panels b−d of Figure 3 represent two critical moments during particle adsorption. After immersion in the gold nanoparticle solution for 4.5 h, adsorption occurs initially in the gap areas (compare panels b and b′ of Figure 3). The resulting images no longer exhibit the distinct domain features, instead, becoming more uniform with nanoparticles inlaid and attached to the DODAM bilayer. With a longer immersion time of 12−14 h (Figure 3c), particles filled all the void space at the interface, forming a layer of gold particles with a more uniform appearance that resembles the underlying gold substrate.

Interestingly, the best agreement between the simulation of the ellipsometric angles $\Delta$ and $\Psi$ with the experimental data gave optical constants ($n$, $k$) for the calculations of the complex refractive index, $N$, of the particle layer, close to the typical values for bulk gold[10] (Table 1). This is in direct contrast to results reported previously by Schiffrin and co-workers.[11] They found that the refractive indexes of nanoparticle films immobilized on organic dithiol monolayers on glass in all cases were *very different* from that of bulk gold values ($n = 2.63$, $k = 1.55$). Furthermore, Schiffrin's values were only slightly influenced by the physicochemical nature of the organic linker. There are two differences between the two systems: the nature of the coupling force immobilizing the particles, and the substrate the particles were adsorbed on. The Schiffrin nanoparticle film was prepared on glass substrates, while the present system utilizes gold substrates. The proximity of gold nanoparticles to a gold film may be the reason for the difference in optical constants between the two systems. Support for this mechanism comes from the formation of nanoparticle aggregates in the bulk by mixing their solution with that of bis-benzamidines. We found significant shifts of the gold plasmon absorption, as reaction progressed. We attributed this to electronic interactions among gold nanoparticles in the aggregates. If similar interactions occur between gold nanoparticle and the gold substrate, changes in the refractive index are to be expected.

The successful formation of each layer of the nanocomposite was further confirmed by external reflection Fourier transform infrared spectroscopy (ER-FTIR, Figure 4).[12] The ER-FTIR spectrum obtained of the MHA SAMs (A) is in accordance with the literature, indicating a complete monolayer formation.

Spectra B−D confirm the adsorption of the bis-benzamidines (PAM, OAM, and DODAM) in qualities as expected from the ellipsometric data. Thus, the bands $\nu(CH_2)_{as}$ at 2945 $cm^{-1}$ and $\nu(C{-}C)_{arom}$ at 1611 $cm^{-1}$ are characteristic for the bis-benzamidines.[5,6] The positions of the $CH_x$ stretching bands indicate a solidlike order of the amidine (MHA/DODAM, spectrum D, $\nu(CH_2)_{as}$ 2917−18 $cm^{-1}$; $\nu(CH_2)_s$ 2849−50 $cm^{-1}$) and the MHA monolayer.

(10) Complex refractive index $N$ of bulk Au at $\lambda = 632.8$ nm ($N = n - ik$) with $n = 0.166$ and $k = 3.15$ from: Palik, E. D., Ed. *Handbook of Optical Constants of Solids*; Academic Press: Orlando, FL, 1985. Or recently, $n = 0.197$; $k = 3.45$ from: Innes, R. A.; Sambles, J. R. *J. Phys. F: Met. Phys.* **1987**, *17*, 277.

(11) Brust, M.; Bethell, D.; Kiely, C. J.; Schiffrin, D. J. *Langmuir* **1998**, *14*, 5425−5429. (b) Baum, T.; Bethell, D.; Brust, M.; Schiffrin, D. J. *Langmuir* **1999**, *15*, 866−871.

(12) Infrared spectra were recorded on a Magna 760 spectrometer from Nicolet equipped with a MCT-A detector cooled with liquid nitrogen and a sample compartment purged with $CO_2$ and moisture-free air. Specta were recorded at 2 $cm^{-1}$ resolution in transmission mode accumulating 200 scans. Solid samples of modified nanoparticles were prepared as a KBr pellet. The monolayer spectra of the self-assembled monolayers were recorded by external reflection FTIR additionally using a SpectraTech FT-80 grazing angle setup at 80° angle of incidence in p-polarization.

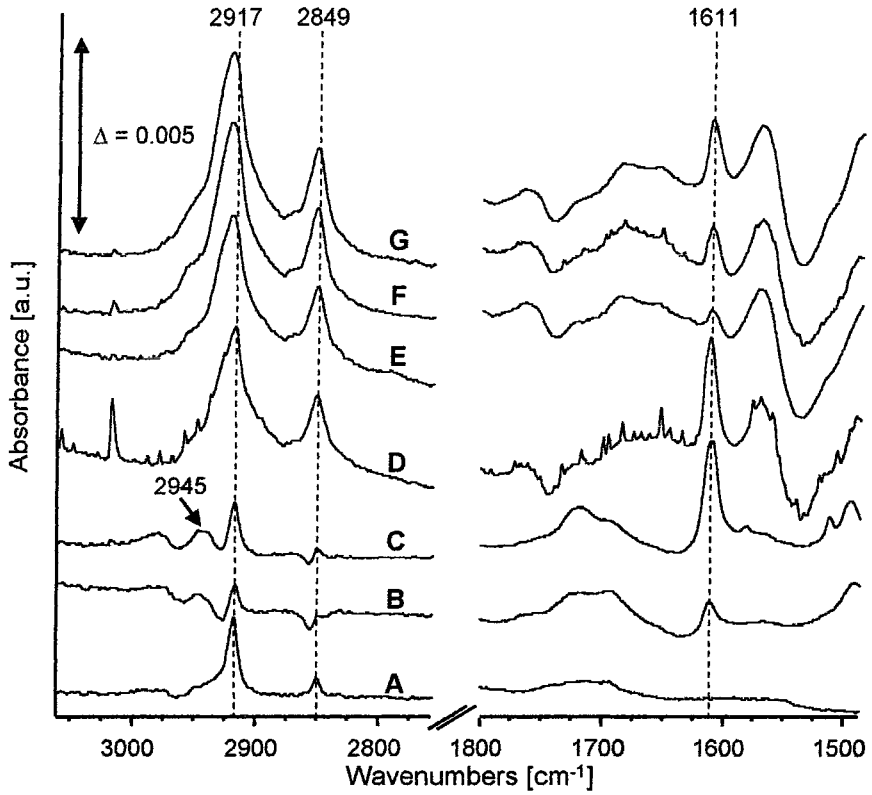


**Figure 4.** ER-FTIR spectra of MHA SAM directly on gold (A), after modification with PAM (B), after modification with OAM (C), after modification with DODAM (D). ER FTIR spectra of MUA-modified gold nanoparticles subsequently adsorbed on Au/MHA/PAM (E), on Au/MHA/OAM (F), and on Au/MHA/DODAM (G). Peak assignments were as follows for G: $\nu(CH_2)_{as}$, 2921 $cm^{-1}$; $\nu(CH_2)_s$, 2851 $cm^{-1}$; $\nu(CC)_{arom}$, 1612 $cm^{-1}$ (in plane). Infrared spectra were recorded on a Magna 760 spectrometer from Nicolet equipped with a MCT-A detector cooled with liquid nitrogen and a sample compartment purged with $CO_2$ and moisture-free air. Spectra were recorded at 2 $cm^{-1}$ resolution accumulating 2000 scans using a SpectraTech FT-80 grazing angle setup at 80° angle of incidence in p-polarization.

After the MUA/nanoparticle adsorption (spectra E to G), however, $CH_x$ stretching bands are much more intense and broader and the band maximum is shifted to higher wavenumbers (2921 and 2850 $cm^{-1}$). The methylene groups of the alkanoic acid shell of the nanoparticle are more disordered than the methylene groups of the MHA/bisamidine bilayers. The high curvature of the gold nanoparticle prevents efficient packing of the methylene units relative to their packing on a planar gold surface.[1d] As seen in the spectra E−G, even after complete particle adsorption, the characteristic adsorption patterns for the bis-benzamidines, especially the $\nu(C-C)_{arom}$ around 1611 $cm^{-1}$, is nearly unaffected and hence indicates that the linking bis-benzamidine layer is stable with respect to exchange by the gold nanoparticles.

In summary, SAMs of bis-benzamidines were found efficient as linking layers between a negatively charged MHA surface and a layer of negatively charged MUA/nanoparticles. The bis-amidine linker could control the particle layer thickness. Furthermore, fitting of the ellipsometric optical values was only possible using a refractive index close to the value of bulk gold for the top particle layer. The concept of using bis-benzamidines of various lengths as linkers and spacers for charged nanoparticles to form bulk 3D crystal-like nanocomposites will be the subject of an upcoming account.[13]

**Acknowledgment.** The authors gratefully acknowledge financial support from the Deutsche Forschungsgemeinschaft (SE 777/2-4) and Deutscher Akademischer Austauschdienst, DAAD (D/98 22606). Funding from the NSF through the MRSEC for Polymers at Engineered Interfaces and the NSF/GRT program (DGE 955452) is gratefully acknowledged. R.J. is thankful for a postdoctoral stipend from the Deutsche Forschungsgemeinschaft.

LA000647X

(13) Auer, F.; Scotti, M.; Jordan, R.; Ulman, A.; Sellergren, B.; White, H.; Rafailovich, M.; Sokolov, J. In preparation.